

(53) **PERFORMANCE OF BIO-ELECTROCHEMICAL REACTOR EQUIPPED WITH A
MULTIPLE-ELECTRODE SYSTEM**

多重電極を用いた生物電気化学リアクターの脱窒特性

Michal Prosnansky* and Masao Kuroda*

ミハル プロシヤンスキー、黒田 正和

ABSTRACT; Feasibility of laboratory-scale bio-electrochemical reactor (BER) equipped with a multiple-electrode system (multiple BER) for treatment of nitrate-contaminated water was experimentally investigated with special attention to the optimum surface area of cathode. The multiple-electrode system was employed to enlarge the surface area of cathode so that improved reactor performance could be attained because of high contact efficiency among electron donor – H_2 , microorganisms and solution. Hence, the overall removal rate was increased with the increasing number of cathodes. However, the current-denitrification efficiency gradually declined with increasing current density. As a consequence, the electric energy consumption per removed nitrate was increased exponentially with current density. Thus, it was not reasonable to apply high currents for the multiple BER used in this study. An investigation on the optimum specific surface area of cathode, as a function of electric energy consumption, was carried out. Increasing number of cathodes resulted in the Ohmic potential drop due to the increasing distance between anode and cathodes. Also, the surface over-potential increased with the increasing current density. The appropriate specific surface area of cathode for the bio-electrochemical denitrification was estimated.

KEYWORDS; bio-electrochemical reactor (BER), multiple-electrode system, denitrification.

1. INTRODUCTION

A bio-electrochemical reactor (BER) has been studied extensively in recent years. It has usually been equipped with a couple of electrodes and attached biofilm on a cathode. After applying electric current, H_2 and O_2 gasses are produced from cathode and anode, respectively. Hydrogen gas is supplied to bacteria as an electron donor, while nitrate is utilized as an electron acceptor.

Earlier studies have investigated the effect of current and/or current density¹⁰⁾, COD⁵⁾, physical property of electrode and electrode type^{3) 9) 11)} on denitrification rate. In order to develop a practical bio-electrochemical denitrification system, it is necessary to apply a multi-cathode system rather than a single cathode one to enlarge the surface area of cathode in order to increase the reactor performance by maintaining the high contact efficiency among electron donor – H_2 , microorganisms and solution.

Most recently, a multi-electrode system⁸⁾ was proposed. The denitrification rate obtained by the electrode system was so fast that hydraulic retention time (HRT) could be reduced to about 2 hr as a consequence of enlarged effective surface area of electrode and the formation of low ORP zone in the multi-cathode region. The experimental results suggested, however, that the electric power consumption per removed nitrogen increased in multiple BER.

The objective of this study is to investigate the suitability of electrode system for nitrate removal and the appropriate specific surface area of cathode for the multiple BER from the viewpoint of current-denitrification efficiency and energy consumption.

2. MATERIALS AND METHODS

2.1 Bio-electrochemical reactor (BER)

The scheme of the experimental apparatus is shown in Fig. 1. The laboratory-scale reactor was supplied with a solution containing 15 ~ 40 mg-N/l of nitrate, which was fed into the cathodic zone and discharged from BER through the anodic zone.

The multiple BER consisted of 5 sandwich-type cathodes and an inert anode (platinum coated titanium). As shown in Figure 1, each cathode was composed of three layers – stainless steel mesh; granular active carbons (GACs), which were connected with the stainless steel mesh to enlarge the surface area of cathode and to attach bacteria; and porous plexus-glass wall, which was used to prevent the contact among cathodes. The size of cathode was: width = 10 cm, height = 15 cm and thickness = 0.8 cm. The diameter of a GAC granule was 4 mm in average. The distance between stainless steel meshes was 1.0 cm and between the downstream cathode and the anode 2.5 cm.

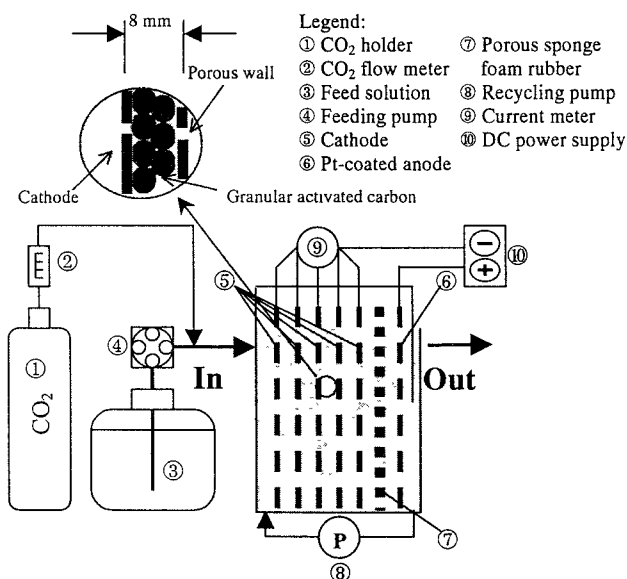


Fig. 1. Experimental apparatus used in this study.

between the cathodic and the anodic zone to prevent the mixing of H₂ and O₂ bubbles produced by the electrolysis of water. BER was operated in a flow-through mode, where water flowed through the openings in electrodes with size of several mm. The volume of BER was 1.2 l with a void volume of 0.6 l. The effective surface area of each electrode was considered as a cross-sectional area of electrochemical cell. The total surface area of the cathode and the anode was 750 cm² and 150 cm², respectively.

2.2 Analytical methods

Analyses were performed on daily basis. Nitrate and nitrite concentrations were measured by an ion chromatograph (IC 7000 Series II, Yokogawa Analytical Systems). ORP and pH were measured by an ORP/pH meter (UC 23, Central Kagaku). Dissolved oxygen was analysed by a DO meter (UC 12, Central Kagaku) and the conductivity by a conductivity meter (SE 12, Horiba).

We expect that part of H₂ gas could be produced from GACs since they were packed with stainless steel mesh. Hence, H₂ gas could be directly supplied to the denitrifying microorganisms. To increase the H₂ gas production rate from GACs, GACs were placed downstream and stainless steel mesh upstream. Thus, distance between GACs layer and anode was smaller than between stainless steel mesh and anode, which brought about lower Ohmic potential drop in case of GACs.

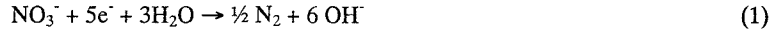
The cathodes were connected in series with the anode. Electric current density of each cathode was controlled independently and the same current density was delivered to each cathode. Current density was defined as electric current divided by the cross-section of reactor ($A = 150 \text{ cm}^2$).

Porous sponge-foam rubber was placed

3. RESULTS AND DISCUSSION

3.1 BER performance

Figure 2 shows the performance of the studied multiple BER. The experiment was conducted in eight runs. In each run, for the set current density and the influent concentration of nitrate, an appropriate HRT was adjusted according to the overall denitrification reaction in BER as follows:



At the beginning of experiment, the effluent concentration of NO_3^- exceeded that of WHO guideline for drinking water ($\text{NO}_3^- \leq 10$ mg-N/l). The reason was high pH ($\text{pH} = 9 \sim 12$) due to the production of OH^- in the cathodic region (see reaction (1)). CO_2 was thereby fed into the system to keep pH around neutrality. It promptly resulted in an improved quality of effluent in Run 1 with the average effluent NO_3^- concentration of around 5.0 mg-N/l. NO_2^- was often detected in Run 1 (Fig. 2), but it was no longer detected once pH was corrected.

From Runs 2 to 5, the influent NO_3^- concentration was reduced in step-wise manner to maintain the effluent $\text{NO}_3^- \leq 10$ mg-N/l. Also HRT was reduced with increasing current density from 6 hr in Run 1 to 20 min in Run 6 (see Fig. 2). The denitrification rate in Run 1 through 6 was 3.7, 5.6, 5.9, 6.8, 11.3 and 10.4 mg-N/hr, respectively. The denitrification rate was increasing with increasing electric current and decreasing HRT, until it reached the maximum in Run 5. Then the denitrification rate and the concentration of decomposed NO_3^- started to decline (Fig. 2) due to the decreasing current-denitrification efficiency discussed in detail in section

3.3.

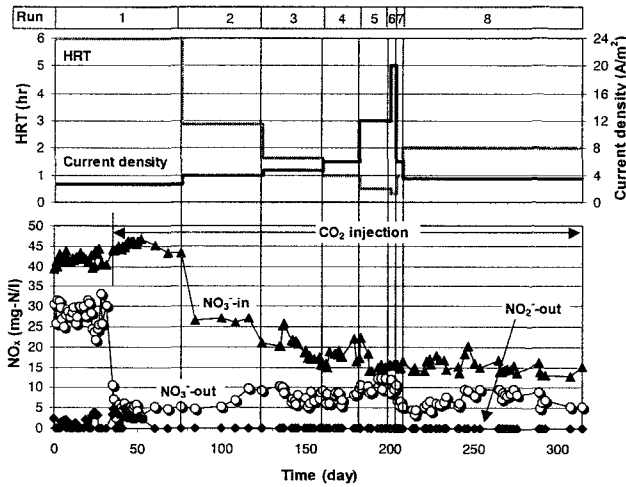
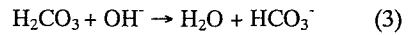
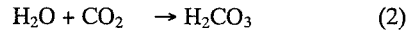


Fig 2. Time course change of effluent NO_3^- and NO_2^- in BER equipped with the multiple electrode system.

3.2 Role of CO_2 in multiple BER

As it was already mentioned, CO_2 gas was injected into the cathodic zone to buffer pH. The produced OH^- reacts with CO_2 consistent with the following reactions:



Since the target pH was 7, the production of CO_3^{2-} could be neglected and thus it was not considered in the calculation. According to the reactions (1) through (3) we can calculate CO_2 feeding rate [mmol/sec]:

$$J_{\text{CO}_2} = \frac{6A}{5\alpha F} i \quad (4)$$

where α is:

$$\alpha = \left(1.0 + \frac{C_{\text{H}^+}}{K_1} + \frac{K_2}{C_{\text{H}^+}} \right)^{-1} \quad (5)$$

A is the cross-sectional area of electrochemical cell ($A = 0.015 \text{ m}^2$), α is the fraction of HCO_3^- in total CO_3 species [-], F is Faraday constant [C/mol], i is current density [A/m^2], C_{H^+} is the concentration of H^+ ($C_{\text{H}^+} = 10^{-7} \text{ mol/l}$), K_1 and K_2 are the dissociation constants of carbon dioxide and bicarbonate, respectively ($K_1 = 4.4 \times 10^{-7}$ and $K_2 = 4.69 \times 10^{-11}$)¹²). The feeding of CO_2 , as a function of current density, is shown in Fig. 3. Eq. (4) is represented by the solid line and the measured experimental values by the square points. Fig. 3

demonstrates a very good agreement between the calculated and the measured values and thus confirms the validity of Eq. (4).

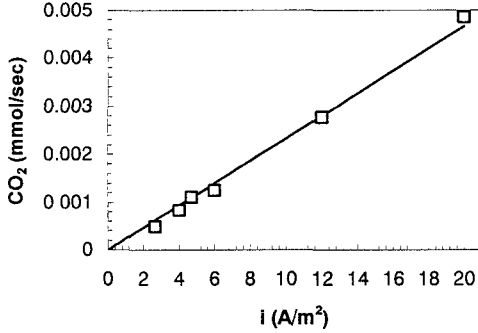


Fig. 3. CO₂ gas feeding rate.

This electrolyte does not only buffer pH but also can carry electric current as H⁺ and/or OH⁻ do. OH⁻ produced at cathode is captured instantaneously by CO₂ and carried by HCO₃⁻⁸⁾. Hence, the conductivity of the solution is improved due to the CO₂ feeding, which is expressed by the following equation:

$$\kappa = \kappa_0 + \Lambda_{HCO_3^-} C_{HCO_3^-} \quad (6)$$

where κ_0 is the conductivity of influent ($\kappa_0 = 0.21$ mS/cm), $\Lambda_{HCO_3^-}$ is molar conductivity of HCO₃⁻. For a dilute solution we can approximate $\Lambda_{HCO_3^-} \approx \Lambda_{HCO_3^-}^0$ ($\Lambda_{HCO_3^-}^0$ is molar conductivity at infinite dilution = 41.5 S m²/mol). $C_{HCO_3^-}$ is the concentration of HCO₃⁻, which is defined as follows:

$$C_{HCO_3^-} = \alpha \cdot \frac{J_{CO_2}}{Q} \quad (7)$$

where Q is the volumetric flow rate (cm³/s).

3.3 Current-denitrification efficiency and denitrification rate

The current-denitrification efficiency (ϕ) was calculated based on the measured values of volumetric flow-rate, influent and effluent concentrations of NO₃⁻ ($C_{NO_3^-}^{in}$ and $C_{NO_3^-}^{out}$), as well as the total current (I_T). It was calculated from the following equation based on reaction (1):

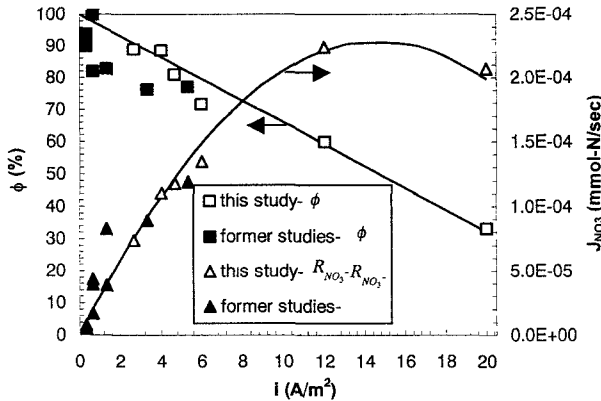


Fig.4. Current-denitrification efficiency and denitrification rate.

$$\phi = \frac{Q(C_{NO_3^-}^{in} - C_{NO_3^-}^{out})}{I_T / 5F} \quad (8)$$

where $C_{NO_3^-}^{in}$ and $C_{NO_3^-}^{out}$ are the influent and the effluent concentrations of NO₃⁻, respectively [mol/cm³], I_T is the total current [A].

The relationship between the configuration of electrodes and the operating conditions on ϕ are far too complex for exact expression. Hence, we estimated the trend of the current-denitrification efficiency from a linear regression of Eq. (8) expressed as a function of the current density and number of electrodes (n):

$$\phi = 1 - \frac{0.17}{n} i \quad (9)$$

Based on Eq. (9), ϕ varies with the changing current density. Thus, we can observe that ϕ is gradually declining with increasing current density. The calculation was verified by ϕ attained in the former BER studies ^{1) 2) 4) 7) 8)}.

The overall denitrification rate ($R_{NO_3^-}$) was expressed by the following equation [mmol-N/sec]:

$$R_{NO_3^-} = \sum_{j=1}^n \frac{A i_j \phi}{5F} = \frac{I_T \phi}{5F} \quad (10)$$

where i_j is the electric current density of electrode couple j [A/m²].

When electric current is increased, the H₂ gas production is enhanced. Therefore, one can also expect enhanced NO₃⁻ removal according to Reaction 1. This would be true, if the removal efficiency was 100%. Since the current-denitrification efficiency declined with the rising current, as it was mentioned above, $R_{NO_3^-}$ was smaller than expected by Reaction 1 (see Eq. (10) and Fig. 4). Moreover, we can observe from Fig. 4 that $R_{NO_3^-}$ started to decline after the current-denitrification efficiency dropped below 50%. The decline of $R_{NO_3^-}$ may be explained by the inhibition of bacterial activity due to high pH at the surface of cathode under high current densities. Thus, bacteria did not utilize part of the produced H₂ gas, which suggests that it was not reasonable to apply high current for multiple BER used in this study.

3.4 Energy consumption

Energy consumption, or requirement to treat a unit concentration of nitrate, was expressed by:

$$W_T = \frac{A}{R_{NO_3^-}} \sum_{j=1}^n \varepsilon_j i_j = \frac{5F}{n\phi} \sum_{j=1}^n \varepsilon_j \quad (11)$$

where W_T is the total energy consumption [J/mol-N], ε_j is the electric potential drop between anode and cathode j [V].

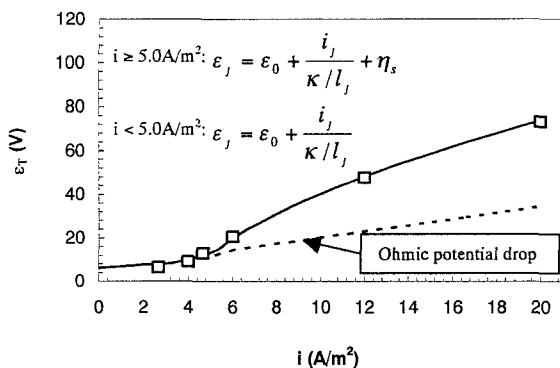


Fig. 5. Total electric potential.

proceed at an appreciable rate ⁶⁾. We assumed that η_s is a difference between the Ohmic potential and the experimental values (see Fig. 5). A logarithmic function was chosen to correlate the experimental values since η_s typically has a logarithmic characteristic ⁶⁾:

$$\eta_s = a + b \log i \quad (14)$$

The electric potential drop is comprised of the potential of water electrolysis ($\varepsilon_0 = 1.2$ V), the Ohmic potential drop and the surface over-potential (η_s), as follows:

$$\varepsilon_j = \varepsilon_0 + \frac{i_j}{\kappa / l_j} + \eta_s \quad (12)$$

$$\varepsilon_T = \sum_{j=1}^n \varepsilon_j \quad (13)$$

where l_j is the length from cathode j to anode [m] and ε_T is the total potential drop [V]. The surface over-potential, an additional contribution to the overall cell potential dependent on the property of electrochemical cell, is a driving force required to make the electrode reactions

where a and b are constants ($a = -45$ and $b = 65$) estimated by the interpolation of experimental results shown in Fig. 5 with Eq. (14).

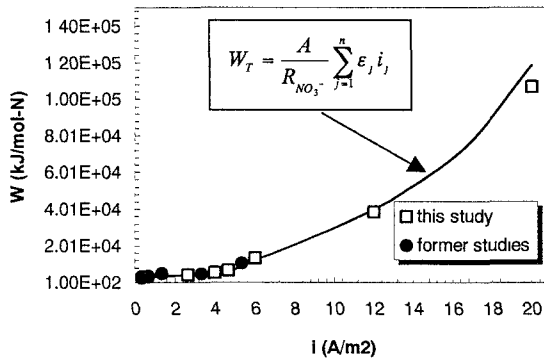


Fig. 6. Energy consumption.

shown in Fig. 6. The energy consumption rises exponentially due to the declining removal efficiency (see Eq. (11)). The calculation was compared with the experimental values observed in this study as well as with those obtained in the former BER studies ^{1) 2) 4) 7) 8)}. Fig. 6 demonstrates a very good agreement between the calculated and observed values. Since higher current densities were not used in the former BER studies, we could not compare the calculation in wide range.

3.5 Optimum specific surface area of cathodes

The specific surface area of cathode (a) was investigated by relating it with the current-denitrification efficiency and electric energy consumption, since they directly indicate the operating cost of the process. The specific surface area of cathodes was defined as a number of cathodes multiplied by the cross-sectional area of reactor and divided by the volume of reactor. The optimum specific surface area of cathode was investigated for the following input data: total current - $I_T = 10; 60; 90; 120; 180; 250; 300$ mA and influent nitrate concentration - $C_{NO_3^-}^{in} = 15$ mg-N/l. The same type of multiple BER with the same dimensions and distances among electrodes as in the experiment was considered. According to the experiment, it was also assumed that each cathode would be controlled independently, and the same electric current would be applied for each couple of electrodes. The investigation was carried out for the number of cathodes ranging from 1 to 16. The current-denitrification efficiency was estimated from Eq. (9) for each set of conditions (different electric current and different number of cathodes), denitrification rate from Eq. (10), the energy consumption was calculated from Eq. (11), electric potential from Eq. (12) ~ (14). The parameters in Eq. (9) and (14), respectively, were regarded as the same as in the previous sections. The calculation was verified by the efficiency and energy consumptions achieved in this study and in the former BER studies ^{1) 2) 4) 7) 8)}. The result illustrated in Fig. 7 shows a good agreement between the calculated and the measured values, and thus confirms the validity of calculation.

The current-denitrification efficiency depends on two factors: total current and specific surface area of cathodes. As shown in Fig. 7, with increasing electric current, the efficiency decreased, on the other hand, the larger specific surface area resulted in higher efficiency. Both outcomes can be explained by Eq. 9. Increasing specific surface area is reflected in larger surface area of cathodes and consequently in decreasing current density. Furthermore, enlarged specific surface area of cathode increases the contact efficiency among electron donor – H_2 , biofilm and solution. Hence, increasing specific surface area of cathode improves the current-denitrification efficiency.

The decreasing contact between solution and electrodes caused the development of surface over-potential, which was probably associated with H_2 production. At low current densities, the H_2 generation is low and therefore H_2 is dissolved in water. However, at higher current densities, the H_2 production rate increases and the generated H_2 starts to form bubbles. If current density is increased further, size of bubbles increases. In Fig. 5, ϵ_r started to deviate from the Ohmic potential drop at $i > 5.0$ A/m² when H_2 gas utilization rate decreased below 80% because part of the produced H_2 bubbles began to get trapped in biofilm, which brought about a decrease of the contact between solution and electrodes.

The evolution of energy consumption is

Increasing number of cathodes caused a rise in the Ohmic potential drop due to the increasing distance between the anode and the cathodes. On the other hand, the increasing number of cathodes resulted in enlarged surface area of cathode and consequently in lower cathodic current density, which positively affected the current-denitrification efficiency. These two opposing factors caused that the energy consumption reached its minimum at higher number of cathodes with increased electric current. The minimum energy consumption is represented by the bold solid line in Fig. 7.

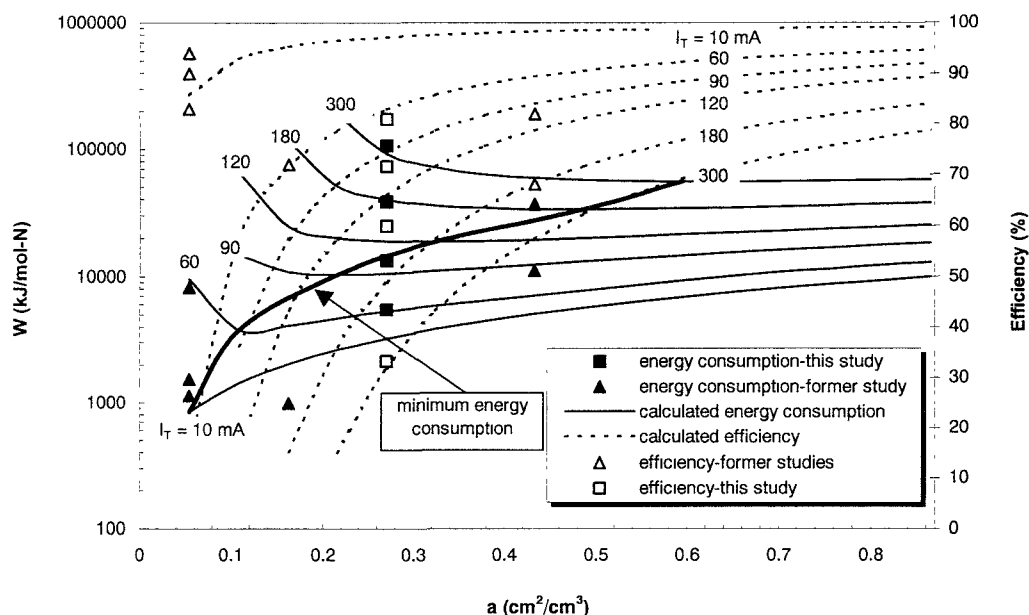


Fig.7. Current-denitrification efficiency and energy consumption dependent on the number of cathodes inserted into BER.

4. CONCLUSIONS

A bio-electrochemical reactor equipped with a multiple-electrode system was investigated using a laboratory-scale apparatus for a treatment of nitrate-contaminated water. The following results were obtained:

- (1) A multi-cathode system was employed rather than a single cathode one to enlarge the surface area of cathode in order to increase the reactor performance by maintaining the high contact efficiency among electron donor – H_2 , microorganisms and solution. Hence, the overall removal rate was increased with the number of cathodes. However, the current-denitrification efficiency gradually decreased with increasing current density. As a consequence, the electric energy consumption per removed nitrate exponentially increased with increasing current density. Thus, it was not reasonable to apply high currents for the multiple BER used in this study.
- (2) An investigation on the optimum specific surface area of cathode, regarded as a function of electric energy consumption, was carried out. Increasing number of cathodes caused a rise in the Ohmic potential drop due to the increasing distance between anode and cathodes. Also, the surface over-potential increased with increasing current density. Based on which the appropriate specific surface area of cathodes for the bio-electrochemical denitrification was estimated.

REFERENCES

1. Feleke Z., Araki K., Sakakibara Y., Watanabe T. and Kuroda M. (1998) Selective reduction of nitrate to nitrogen gas in a biofilm-electrode reactor. *Wat. Res.* 32(9), 2728-2734.
2. Flora R. V., Suidan M. T., Islam S., Biswas P. and Sakakibara Y. (1993) Numerical modelling of a biofilm-electrode reactor used for enhanced denitrification. *2nd International Specialized Conference on Biofilm Reactors*, 613-620.
3. Guo Y., Watanabe T. and Kuroda M. (1997) Denitrification of nitrate polluted water by using a bio-electro rotating contactor. *Proceeding of Environmental Engineering Research* 34, 155-162.
4. Islam S. and Suidan M. T. (1998) Electrolytic denitrification: Long term performance and effect of current intensity. *Wat. Res.* 32(2), 528-536.
5. Kuroda M., Watanabe T. and Umedu Y. (1997) Simultaneous COD removal and denitrification of wastewater by bio-electro reactors. *Wat. Sci. and Tech.*, 35(8), 161-168.
6. Newman J. S. (1991) Electrochemical systems – second edition. *Prentice Hall*, 16-25.
7. Sakakibara Y., Araki K., Watanabe T. and Kuroda M. (1997) The denitrification and neutralisation performance of an electrochemically activated biofilm reactor used to treat nitrate-contaminated groundwater. *Wat. Sci. and Technol.* 36(1), 61-68.
8. Sakakibara Y. and T. Nakayama (2001) A novel multi-electrode system for electrolytic and biological water treatments: electric charge transfer and application to electric charge transfer and application to denitrification. *Wat. Res.* 35(3), 768-778.
9. Tanaka T., Watanabe T. and Kuroda M. (1998) Estimation of nitrification enhanced by application of electric current. *J. of Japan Society on Water Environment*, 21, 596-602.
10. Watanabe T., Motoyama H. and Kuroda M. (2001) Denitrification and neutralization treatment by direct feeding of an acidic wastewater containing copper ion and high-strength nitrate to a bio-electrochemical reactor process. *Wat. Res.*, 35(17), 4102-4110.
11. Zhe-shi Z., Ozeki M. and Kuroda M. (1997) Denitrification of nitrified wastewater by bio-electro process. *J. of Japan Society on Water Environment*, 20, 481-485.
12. Saweyr C.N., McCarty P.L. and Parkin G.G. (1994) Chemistry for environmental engineering, *McGraw-Hill, Inc.*, 30-40.